

Monte Carlo Calculations of High-Energy Nuclear Interactions. I. Systematics of Nuclear Evaporation*

I. DOSTROVSKY, *Brookhaven National Laboratory, Upton, New York, and The Weizmann Institute of Science, Rehovoth, Israel,*
P. RABINOWITZ, *The Weizmann Institute of Science, Rehovoth, Israel,*

AND

R. BIVINS,† *Los Alamos Scientific Laboratory, University of California, Los Alamos, New Mexico*

(Received March 31, 1958)

The process of nuclear de-excitation by evaporation has been calculated by using a Monte Carlo method and fast electronic computers. The competition between the emission of neutrons, protons, deuterons, tritons, He³, and He⁴ has been studied as a function of various parameters and experimental conditions. A systematic survey is presented for a range of atomic numbers, mass numbers and excitation energy of initial nuclei. The nuclides studied extend from $A=49$ to $A=239$ with $Z=Z_A\pm 3$. The range of excitation energies for which computations are presented extends from 100–700 Mev. Among the parameters affecting the process the importance of the temperature correction of the Coulomb barrier and the level density parameters are considered in detail. The average properties of the process such as average numbers of the various particles emitted, the average number of nucleons, of charged particles, and of charges emitted are summarized in graphical and tabular form for various combinations of the parameters used in the computation. Energy spectra of the various emitted particles are also shown.

I. INTRODUCTION

IN the interpretation of the results of the interactions of high-energy particles with matter, it is found necessary at some point, irrespective of the mechanism adopted for the interaction, to consider the fate of a highly excited nucleus. In the range of excitations considered here, particle emission is the only effective process for de-excitation. This process, known commonly as the evaporation process, has been studied by a number of authors, notably by LeCouteur¹ and Fujimoto and Yamaguchi.² The treatment of these authors is based on the statistical model of the nucleus and starts essentially from the formula of Weisskopf,³

$$P_j(T)dT = \gamma_j \sigma T [\rho(f)/\rho(i)] dT, \quad (1)$$

where $P(T)dT$ is the probability per unit time of emission of a particle j with kinetic energy in dT , σ is the total cross section for capture of particles j by the final nucleus, $\rho(f)$ and $\rho(i)$ are the level densities of the final and initial nuclei, respectively, and are functions of mass, charge, and excitation energy. $\gamma_j = gm/\pi^2 \hbar^3$, where g is number of spin states and m mass of particle j .

From this fundamental equation it is possible after assuming an explicit model for the nucleus, Fermi gas in this case, to calculate the relative probability of emission of various types of particles j from a given nucleus and excitation. In practice what is required are the integrated probabilities over the whole of the de-excitation process. Such an integration has been

attempted by LeCouteur¹ and Fujimoto and Yamaguchi² and for excitations below 100 Mev by Jackson,⁴ but was found possible only after severe approximations and after assuming stationary values for some of the variables.

In the present calculations the step-wise Monte Carlo method has been adopted for following the fate of a given excited nucleus, and the average behavior has been deduced from an analysis of a large number of complete evaporation cascades. This procedure does not require any averaging approximations since the various probabilities are recalculated afresh after the emission of each individual particle. A similar procedure has recently been described by Rudstam.⁵

In the present paper we report the systematic study of the effect of various parameters on the evaporation process. The results, while providing one with a general feel of the subject and laying the basis for extrapolation to regions outside the limited field studied, are not directly applicable to computation of specific high-energy interactions. For the latter purpose we require in addition to information on the evaporation process also knowledge of the products of the prompt knock-on cascade⁶ and of competition by fission.⁷ Further papers in this series will deal with the computation of specific interactions and comparison with experiment.

The nuclei and parameters studied in this paper were chosen to illustrate the effect of changing atomic number, mass number, excitation energy, level density parameter, and Coulomb barrier on the evaporation

* This work was supported in part by the U. S. Atomic Energy Commission.

† Now at the University of Illinois, Urbana, Illinois.

¹ K. J. LeCouteur, Proc. Phys. Soc. (London) **A63**, 259 (1950).

² Y. Fujimoto and Y. Yamaguchi, Progr. Theoret. Phys. (Japan) **4**, 468 (1950); **5**, 76 (1950); **5**, 787 (1950).

³ V. Weisskopf, Phys. Rev. **52**, 295 (1937).

⁴ J. D. Jackson, Can. J. Phys. **34**, 767 (1956).

⁵ G. Rudstam, thesis, Uppsala, 1956 (unpublished).

⁶ Friedlander, Miller, Metropolis, Bivins, Storm, and Turkevich (private communication); Bull. Am. Phys. Soc. Ser. II, **2**, 63 (1957); N. Metropolis *et al.*, Phys. Rev. **110**, 204 (1958).

⁷ Dostrovsky, Fraenkel, and Rabinowitz, *Proceedings of the Second International Conference on the Peaceful Uses of Atomic Energy, Geneva, 1958.*

cascade. In addition a comparison was made of the effect of using different mass formulas in the computations.

II. EQUATIONS AND PARAMETERS

In the calculations described below equations similar to those derived by LeCouteur¹ were used. From the fundamental equation of the statistical model for a degenerate Fermi gas [Eq. (1)] the following expressions for the relative probability of emission of two particles i , j , are derived [see reference 1, Eq. (62)]:

$$\frac{P_i}{P_j} = \frac{\gamma_i}{\gamma_j} \left(\frac{R_i}{R_j} \right)^{\frac{1}{2}} \frac{a_j}{a_i} \exp\{2[(a_i R_i)^{\frac{1}{2}} - (a_j R_j)^{\frac{1}{2}}]\}, \quad (2)$$

if Bethe's⁸ level density formula is used, and if the simpler Weisskopf³ formula is used:

$$\frac{P_i}{P_j} = \frac{\gamma_i}{\gamma_j} \left(\frac{R_i}{R_j} \right)^{\frac{1}{2}} \frac{a_j}{a_i} \exp\{2[(a_i R_i)^{\frac{1}{2}} - (a_j R_j)^{\frac{1}{2}}]\}. \quad (3)$$

In these expressions, a is defined by the statistical model level density formula:

$$\rho(E) = C \exp[2(aE)^{\frac{1}{2}}], \quad (4)$$

and R_j is the maximum value of the excitation which a nucleus may possess after evaporating a particle j .

$$R_j = E_0 - Q_j - V_j, \quad (5)$$

where E_0 is the excitation energy of the nucleus before evaporation, Q_j binding energy of particle j to residual nucleus, and V_j is the Coulomb barrier for particle j appropriately corrected.

Equations (2) and (3) are very similar and the difference in the pre-exponential coefficients is expected to be important only towards the end of the evaporation cascade when the differences between R_i and R_j become significant. Comparative calculations were carried out using both formula and the results are tabulated in Table I and discussed later.

Before developing Eq. (2) further, it is necessary to make some assumptions regarding the dependence of the parameter a on the neutron excess of the nucleus. We shall use the LeCouteur formulation of this dependence, *viz.*:

$$\begin{aligned} a_n^{\frac{1}{2}} &= a^{\frac{1}{2}}(1 - 1.3\theta/A), & a_t^{\frac{1}{2}} &= a^{\frac{1}{2}}(1 - 1/A - 1.3\theta/A), \\ a_p^{\frac{1}{2}} &= a^{\frac{1}{2}}(1 + 1.3\theta/A), & a_{\text{He}^3}^{\frac{1}{2}} &= a^{\frac{1}{2}}(1 - 1/A + 1.3\theta/A), \\ a_d^{\frac{1}{2}} &= a^{\frac{1}{2}}(1 - 1/2A), & a_\alpha^{\frac{1}{2}} &= a^{\frac{1}{2}}(1 - 3/2A), \end{aligned} \quad (6)$$

where $\theta = (N - Z)/A$.

⁸ H. A. Bethe, *Revs. Modern Phys.* **9**, 69 (1937).

Using Eqs. (5) and (6), one may transform (3) into

$$\begin{aligned} P_n/P_n &= 1, \\ P_p/P_n &= (R_p/R_n) \exp[(a/R_{np})^{\frac{1}{2}}(Q_n - Q_p \\ &\quad - V_p + 5.2\theta R_{np}/A)], \\ P_d/P_n &= 3(R_d/R_n) \exp\{(a/R_{nd})^{\frac{1}{2}}[Q_n - Q_d \\ &\quad - V_d - (1 - 2.6\theta)R_{nd}/A]\}, \\ P_t/P_n &= 3(R_t/R_n) \exp[(a/R_{nt})^{\frac{1}{2}}(Q_n - Q_t \\ &\quad - V_t - 2R_{nt}/A)], \\ P_{\text{He}^3}/P_n &= 3(R_{\text{He}^3}/R_n) \exp\{(a/R_{\text{He}^3n})^{\frac{1}{2}}[Q_n - Q_{\text{He}^3} \\ &\quad - V_{\text{He}^3} - (1 - 2.6\theta)2R_{\text{He}^3}/A]\}, \\ P_\alpha/P_n &= 2(R_\alpha/R_n) \exp\{(a/R_{n\alpha})^{\frac{1}{2}}[Q_n - Q_\alpha \\ &\quad - V_\alpha - (3 - 2.6\theta)R_{n\alpha}/A]\}, \end{aligned} \quad (7)$$

where $R_{nj}^{\frac{1}{2}} = (R_n^{\frac{1}{2}} + R_j^{\frac{1}{2}})/2$. The modifications necessary if Eq. (2) is used are obvious. It will be noted that Eqs. (7) differ from the equivalent equations presented by LeCouteur in that the binding energies appear explicitly and not in an approximate analytical form. In this way one may use experimental binding energies, as for example those compiled by Wapstra⁹ and Huizenga,¹⁰ or in regions where no experimental data are available, the appropriate semiempirical mass formula may be used to compute the Q 's.

In the early calculations Fermi's mass formula, as modified for computation by Metropolis and Reitwiesner,¹¹ was used. In all later calculations, Cameron's¹² mass table, which had in the meantime become available, was used. A comparison of the effect of the two mass formulas was made and the results are summarized in Table II and discussed later.

The parameters V (Coulomb barrier) and a (level density parameter) present a more formidable problem. The Coulomb repulsion, as calculated from elementary electrostatics is not directly applicable to the computation of reaction barriers but must be corrected in several ways. The first and best understood correction is for the quantum-mechanical phenomenon of barrier penetration (or tunneling effect). Several calculations of barrier penetrability are available; however, we shall follow LeCouteur again and use the data of Bethe⁸ and Bethe and Konopinski¹³ in the form of a coefficient k_j multiplying the calculated Coulomb potential.

Thus,

$$V = k_j V_0, \quad (8)$$

where V_0 is to be calculated from elementary electrostatics. The choice of nuclear radius parameter r_0 is important in this calculation, for it determines the

⁹ A. H. Wapstra, *Physica* **21**, 367 (1955); **21**, 385 (1955).

¹⁰ T. R. Huizenga, *Physica* **21**, 410 (1956).

¹¹ N. Metropolis and G. Reitwiesner, U. S. Atomic Energy Commission Report NP-1980 (unpublished).

¹² A. G. W. Cameron, Atomic Energy of Canada Limited Report CRP-690, 1957 (unpublished).

¹³ H. A. Bethe and E. J. Konopinski, *Phys. Rev.* **54**, 130 (1938).

separation of the centers of the nuclei at contact. We have computed this separation from the equation

$$R=r_0[(A-m)^{\frac{1}{3}}+m^{\frac{1}{3}}], \quad (9)$$

with $r_0=1.3\times 10^{-13}$ cm and m the mass of the emitted particle j . The penetrability coefficients used are: for protons, 0.7; for deuterons, 0.77; for tritons and He^3 , 0.8; and for α particles, 0.83. These coefficients (taken from LeCouteur) were chosen to give a good approximation to the quantum mechanical barrier penetration formula for medium mass nuclei. For the heavy and the light elements, the above coefficients give a poorer approximation. However, as far as the total cross section for the emission of a given particle goes, these coefficients introduce only a small error. The main distortion will be in the low-energy end of the kinetic energy spectrum and for this reason no attempt was made to use the spectra presented at the end of this paper in any quantitative way. A more accurate treatment of these spectra, taking into account an improved barrier penetration calculation, will be presented in a later paper in this series.

The correction for penetration, however, is not the only one which may have to be applied. An excited nucleus undergoes expansion and possesses surface oscillations, both of which phenomena may be expected to reduce the Coulomb barrier. These effects are discussed later.

The remaining parameter in Eq. (6) which needs discussion is the level density parameter a . This parameter has been calculated on the basis of several models, and fitted empirically to the Fermi gas model by several authors using results of low-energy reactions. The values obtained vary greatly. Thus, Bethe⁸ calculates a to be $a=A/11$ (after correcting to our choice of $r_0=1.3\times 10^{-13}$ cm) for the free particle model. Bardeen,¹⁴ for the free-particle model with correlation, deduces a value of $a=A/22$ (corrected to $r_0=1.3\times 10^{-13}$ cm). Weisskopf¹⁵ suggested a formula for a for atoms heavier than mass 60, of the form

$$a=0.85(A-40)^{\frac{1}{2}}.$$

Blatt and Weisskopf,¹⁶ from data on slow neutron capture, deduce values of a for odd nuclei, which in the region of mass 100–200, correspond to $a=A/17$. LeCouteur¹ chose for a the form $a=A/12.4$ as best fitting the energy spectra of Page¹⁷ and Harding, Lattimore, and Perkins,¹⁸ while Fujimoto and Yamaguchi² used a value of $a=A/10.5$ in their calculations. Fong¹⁹ has calculated

a for a range of nuclei from data on fast neutron capture cross section and has concluded that the best agreement is obtained by $a=A/20$. Lang and LeCouteur²⁰ have analyzed all data available for reactions up to 10 Mev, and proposed the following relation between excitation energy and nuclear temperature

$$E=(A/11)\tau^2-\tau+\frac{1}{8}A^{\frac{1}{2}}\tau^{7/3}.$$

However, over the region of A and τ of interest here this equation differs very little from the simpler relation

$$E=A\tau^2/8,$$

which is, of course, equivalent to $a=A/8$. Finally, mention should be made of the recent results of Eisberg, Igo, and Wegner²¹ which appear to require a constant value of a ,

$$a=8 \text{ Mev}^{-1},$$

and later work²² where the Fermi gas model was found incompatible with observations.

In view of this bewildering variety of a values, it was decided to regard it as an adjustable parameter, the best value of which is to be determined by comparison with experiment. In further papers of this series, an attempt is made to establish the effective value of a for highly excited nuclei in this way. Most of the calculations in this paper were carried out using $a=A/10$ and $a=A/20$ in order to illustrate the effect of changing this parameter. A few calculations were also made using a constant value of $a=9 \text{ Mev}^{-1}$.

III. THE COMPUTATION

The Monte Carlo calculation of the de-excitation of nuclei by the evaporation process was programmed first for the Los Alamos MANIAC and later, in an improved form, for the Weizmann Institute WEIZAC. Both computers are fast electronic machines of the Institute of Advanced Studies' type. They differ mainly in the memory unit. The MANIAC I had an electrostatic memory of 1024 40-binary-digit words and WEIZAC has a magnetic core memory of 4096 40-binary-digit words.

The flow sheet of the computation as programmed for the WEIZAC is shown in Fig. 1. The input data for each computation includes the A , Z , and excitation energy of the starting nucleus as well as the number of cascades which are to be followed. In addition, for each set of computations the various parameters to be used and other operational instructions are introduced into the program by a short correction tape. These parameters include the value of the coefficient c in the expression for the level density parameter $a=cA$, the type of

¹⁴ J. Bardeen, Phys. Rev. **51**, 799 (1937).

¹⁵ V. Weisskopf, U. S. Atomic Energy Commission Report MDDC-1175 (U. S. Government Printing Office, Washington, D. C., 1947).

¹⁶ J. Blatt and V. Weisskopf, *Theoretical Nuclear Physics* (John Wiley and Sons, Inc., New York, 1952), p. 372.

¹⁷ N. Page, Proc. Phys. Soc. (London) **A63**, 250 (1950).

¹⁸ Harding, Lattimore, and Perkins, Proc. Roy. Soc. (London) **A196**, 325 (1949).

¹⁹ P. Fong, Phys. Rev. **102**, 434 (1956).

²⁰ J. M. B. Lang and K. J. LeCouteur, Proc. Phys. Soc. (London) **A67**, 586 (1954).

²¹ Eisberg, Igo, and Wegner, Phys. Rev. **100**, 1309 (1955).

²² G. Igo, Phys. Rev. **106**, 256 (1957); see also G. Igo and H. E. Wegner, Phys. Rev. **102**, 1364 (1956), for level density measurement summary.

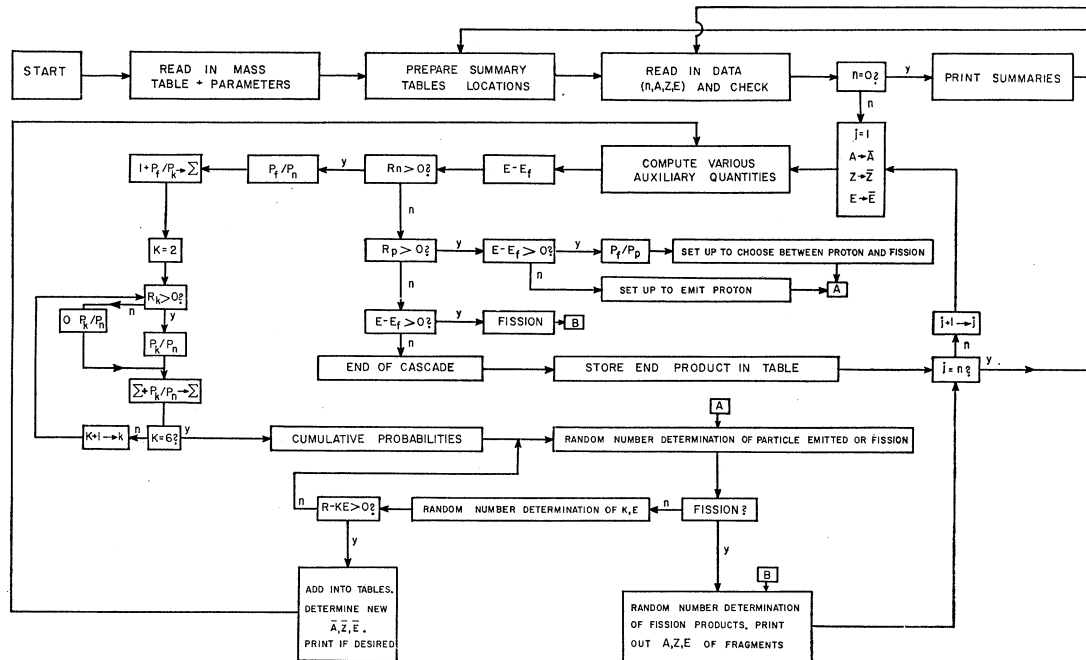


FIG. 1. Flow diagram of evaporation computations, Mk II, (WEIZAC).

Coulomb barrier correction, and the type of print-out desired. Commencing with these data, the relative probability of evaporation of neutrons, protons, deuterons, tritons, He^3 and He^4 were computed using formula (7). From the cumulative sums of these probabilities, normalized to a total 1, the particle to be evaporated was chosen using a pseudo-random number. Weisskopf³ has shown that the kinetic energy of neutrons emitted from a given nucleus followed approximately a Maxwellian distribution. Accordingly, the kinetic energy of the emitted particle was selected from a Maxwellian distribution for the appropriate temperature using a second random number. In case the emitted particle was not a neutron, the appropriate Coulomb barrier was added to the energy selected in this manner. These results were stored away in the memory, the new values of A , Z , and E computed, and the process repeated. The iteration was continued until the initial excitation energy was almost all removed. The exact termination procedure differed somewhat in the MANIAC and WEIZAC calculations. In the first, the process was terminated whenever the residual excitation energy fell below 8 Mev. In the WEIZAC computation, a procedure somewhat closer to physical reality was followed. Iteration was continued so long as any of the R_j 's [Eq. (5)] remained positive. Under these circumstances, it occurred frequently that the kinetic energy chosen by the second random number was greater than the available excitation and in such cases fresh random numbers were computed until a combination was found which permitted the last evaporation to take place. A comparison of the results using the two termination

procedures is given in Tables I and II. It is seen that as far as the average properties of the evaporation process are concerned, the two termination procedures do not lead to significantly different results. Examination of the details of the process however shows that the proportions of protons and α particles evaporated in the last step of the cascade are appreciably higher with the WEIZAC termination. This will effect the energy spectrum of the emitted particles somewhat. The more correct WEIZAC termination will lead to a higher proportion of low-energy protons and α 's than the MANIAC termination.

The program is so arranged that at the completion of the computation of the predetermined number of cascades, the computer summarizes the results, tabulates the spectra, and classifies the products according to their A 's and Z 's. A choice of three types of print-outs is available: (i) Full print-out of each cascade, where at each iteration the nature of the outgoing particle, its kinetic energy and the residual excitation energy of the new nucleus are printed out. At the end of the cascade the final A and Z of the product are printed. (ii) Shorter print-out where only the final A, Z of each cascade is printed out. (iii) only the summaries, spectra and A, Z classification of products is printed out. For most problems this information is sufficient, and since this mode is the most economical in machine time, it was used for most of the computations on the WEIZAC reported in this paper.

The summaries include the following information: the total kinetic energy carried off by each of the six particles, the total de-excitation energy, the total

TABLE I. Comparison of evaporation calculations.^a

	Pa ²³¹ , 450 Mev			Zr ⁹² , 350 Mev		
	MANIAC I	WEIZAC Mk I ^b	WEIZAC Mk II ^c	MANIAC I	WEIZAC Mk I ^b	WEIZAC Mk II ^c
No. of cases	300	76	76	100	52	52
Av No. <i>n</i>	24.3	24.3	24.7	10.1	10.4	10.5
Av No. <i>p</i>	2.8	2.8	2.9	3.9	4.1	4.1
Av No. <i>d</i>	1.0	1.1	0.9	1.4	1.2	1.3
Av No. T	0.4	0.6	0.5	0.5	0.5	0.4
Av No. He ³	0.05	0.07	0.03	0.1	0.2	0.3
Av No. α	1.3	0.9	0.9	1.2	1.1	1.0
Av No. <i>j</i>	29.8	29.8	29.9	17.2	17.5	17.5
Av ΔA	35.6	34.8	34.6	23.5	23.3	23.0
Av <i>j</i> ⁺	5.5	5.4	5.3	7.1	7.1	7.0
Av ΔZ	6.8	6.4	6.0	8.5	8.3	8.2

^a $q = A/10$; temperature-independent Coulomb barrier.

^b No (R_i/R_j) term; proper termination.

^c Equation (3); proper termination.

numbers of each of the six kinds of particles evaporated, the total number of particles, total number of nucleons, total number of charged particles, and total number of charges lost. The last line of the summary is the total number of cascades computed and using this, the average values of all the quantities listed above may be computed. Following these, there are presented the energy spectra of the six particles given for energy intervals of 1 Mev until 35 Mev and thereafter in intervals of 5 Mev. Following the spectra there is printed out the classification of the final products of the evaporation process according to their *A*'s and *Z*'s. The time taken to complete a computation of one cascade varies between 4 and 10 seconds depending upon the initial excitation energy.

Before embarking on the bulk of the calculations, a comparison was made of the effect of using Eqs. (2) or (3) in the computation. The results are shown in Table I. The difference in average properties obtained in the two cases studied appears to be negligible. The difference is expected to be significant toward the end of the cascade only but is insufficient to influence the over-all results. It may be that for very low starting

excitation energies the two equations will differ slightly more but in any case, their validity for low excitation is doubtful. All the early MANIAC calculations were based on Eq. (2) with the term in $(R_i/R_j)^{\frac{1}{2}}$ omitted altogether. The WEIZAC results were based on Eq. (3) unless otherwise specified.

The MANIAC and first WEIZAC programs were based on the Fermi mass formula.¹¹ When later the computation was reprogrammed for use with Cameron's mass table,¹² it became interesting to see to what extent previous calculations are in error due to the approximate nature of the mass formula used earlier. Several comparisons were run and they are listed in Table II. The two examples were chosen to as to compare Fermi's formula with Cameron's tables, both in the region of closed nuclear shells and in region free from shell effect. The evaporation path of Pa²³¹ cuts across both the 82 proton shell and the 126 neutron shell. The evaporation path of Hg²⁰² does not cross any nuclear shells. Correspondingly we see from Table II that in Pa²³¹, appreciable differences occur both in the average properties and in the distribution of products when Cameron's table is used. In the Hg²⁰² case, the differences are very

TABLE II. Comparison of mass formulas in the evaporation calculations.

	Pa ²³¹ , 450 Mev			Hg ²⁰² , 350 Mev		
	MANIAC I	WEIZAC ^a _A	WEIZAC ^b _B	MANIAC I	WEIZAC ^a _A	WEIZAC ^b _B
No. cases	300	100	100	100	100	100
Av No. <i>n</i>	24.3	25.0	23.4	20.1	20.6	19.9
Av No. <i>p</i>	2.8	3.0	3.6	1.9	2.1	2.3
Av No. <i>d</i>	1.0	0.9	1.0	0.6	0.6	0.6
Av No. T	0.4	0.4	0.5	0.3	0.3	0.3
Av No. He ³	0.05	0.03	0.05	0.03	0.02	0.02
Av No. α	1.3	1.0	1.8	0.8	0.7	0.8
Av No. <i>j</i>	29.8	30.4	30.4	23.8	24.3	23.9
Av ΔA	35.6	35.2	37.9	27.4	27.5	27.3
Av <i>j</i> ⁺	5.5	5.4	6.9	3.7	3.7	3.9
Av ΔZ	6.8	6.4	8.8	4.5	4.4	4.7

^a WEIZAC-A: Eq. (3); Fermi mass formula.

^b WEIZAC-B: Eq. (3); Cameron's¹² mass table.

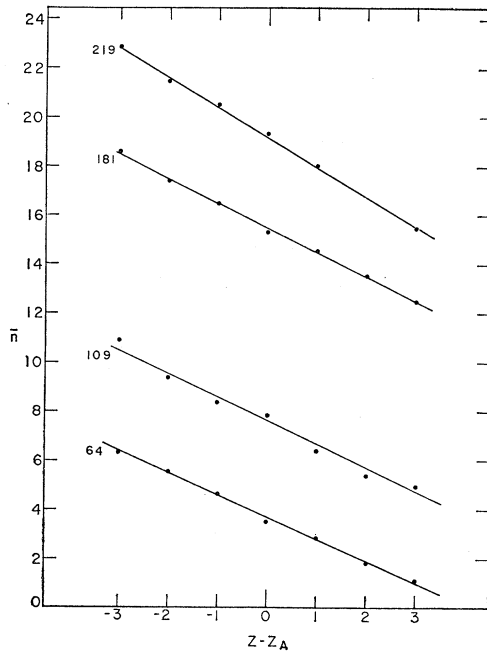


FIG. 2. Average number of neutrons evaporating from members of isobars. Initial nuclear temperature 4 Mev, $a=A/10$, $V=V_0$ (Coulomb barrier independent of excitation).

slight. As expected, the use of the improved mass formula does lead to changes in the results in the shell regions but in the other regions where shell boundaries are not crossed the two formulas lead to the same results. This insensitivity of the computation to the exact form of the mass equation over wide ranges of nuclides is gratifying in that it makes the choice less critical.

Most of the results reported in this paper were obtained using Cameron's mass table.¹² Approximately 4000 masses were packed into about 2000 memory locations to form a working table. Two such mass tables were prepared, one for use with nuclei $Z=94$ to $Z=50$ and the other for nuclei $Z=75$ to $Z=11$.

IV. DEPENDENCE ON Z IN ISOBARS

If attention is confined to the evaporation behavior of members of isobars, a number of simple relationships, useful in interpolations, are found. Within the rather narrow limits of Z studied, i.e., $Z_A \pm 3$, the average numbers of the various particles evaporated are approximately linear in $\Delta Z = Z - Z_A$, for the same initial

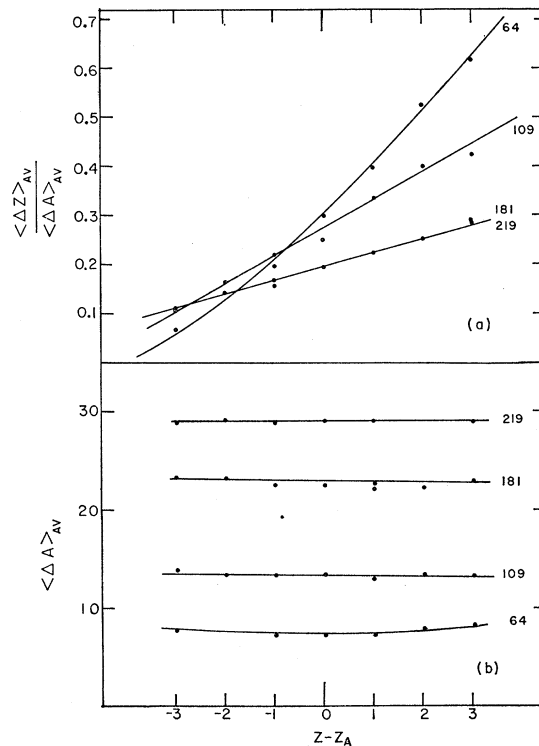


FIG. 3. (a) $\langle \Delta Z \rangle_{Av} / \langle \Delta A \rangle_{Av}$ for the evaporation from members of isobars; (b) $\langle \Delta A \rangle_{Av}$ for same. Initial nuclear temperature 4 Mev, $a=A/10$, $V=V_0$.

nuclear temperature. Similar linear relationships are found for the average number of charges lost. Figure 2 illustrates these points with respect to the average number of neutrons. The parameters of the various lines (obtained by least squares fit) depend somewhat on the A of the isobar. They are summarized for convenience in Table III.

The average number of nucleons lost in the evaporation as well as the emission ratio, i.e., the ratio of doubly charged particles to total charged particles, is found to be almost independent of $(Z - Z_A)$. A corollary of these relations is the linear dependence of the ratio $\langle \Delta Z \rangle_{Av} / \langle \Delta A \rangle_{Av}$ on $(Z - Z_A)$ in an isobar (see Fig. 3).

V. THE DEPENDENCE ON A AND Z

The effect of changing the initial atomic and mass numbers of the excited nucleus was studied at two values of initial nuclear temperature, 4 Mev and 6 Mev. 200 cascades were followed in each case and the

TABLE III. Parameters of lines representing \bar{n} , \bar{p} , $\bar{\alpha}$, as function of $(Z - Z_A)$ for various isobars, for initial nuclear temperature of 4 Mev. $j = C_j + D_j(Z - Z_A)$.

A	C_n	D_n	C_p	D_p	C_α	D_α
64	4.13 ± 0.04	-0.89 ± 0.02	1.60 ± 0.06	0.57 ± 0.03	0.35 ± 0.03	0.09 ± 0.01
109	8.15 ± 0.09	-0.95 ± 0.04	2.00 ± 0.04	0.51 ± 0.02	0.57 ± 0.03	0.08 ± 0.01
181	16.0 ± 0.02	-0.99 ± 0.01	2.30 ± 0.04	0.39 ± 0.02	0.69 ± 0.04	0.08 ± 0.02
219	19.7 ± 0.04	-1.20 ± 0.02	2.50 ± 0.05	0.43 ± 0.02	1.10 ± 0.01	0.17 ± 0.01

starting nuclei were taken at intervals of 10 mass numbers from mass 40 to mass 240. For each mass number three values of Z were taken, one on the stability line (Z_A) and one each on either side of stability and 3 units of Z away (Z_A+3 and Z_A-3). In this way we have for each isobar a comparison of the behavior of neutron-excess and neutron-deficient nuclides.

The results of these computations are presented in Figs. 4-8. The statistics of the rarer particles (D, T, He³, and He⁴) were too poor to justify detailed plotting.

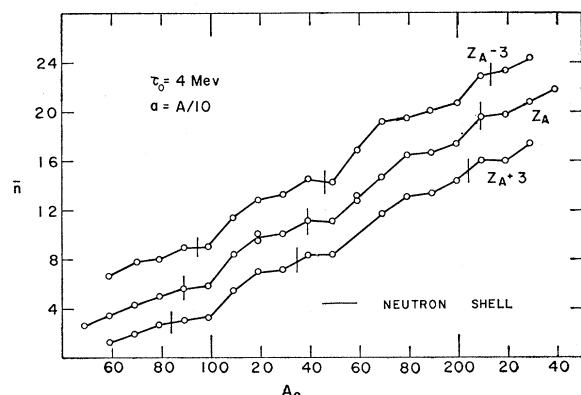


FIG. 4. Average number of neutrons evaporated from different starting nuclei. Initial temperature 4 Mev, $a=A/10$, $V=V_0$.

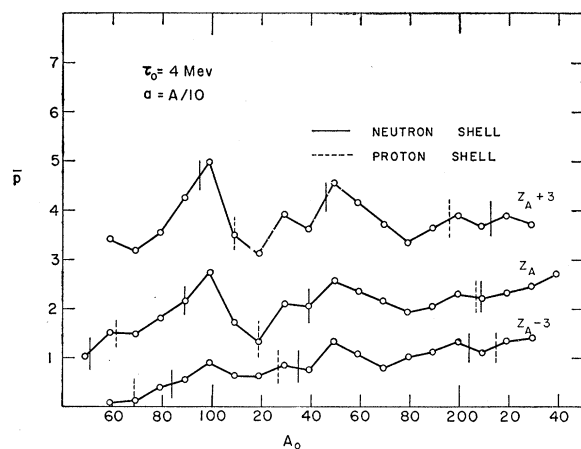


FIG. 5. Average number of protons evaporated from different starting nuclei. Initial temperature 4 Mev, $a=A/10$, $V=V_0$.

The discontinuities and peaks seen in these figures are the expressions of the effects of shell structure of the nuclei on their binding energies. The discontinuities in the plot of the average number of neutrons evaporated against A , the mass number of the initial excited nucleus, occur in the vicinity of mass numbers 210, 140, 90, and 50 and are clearly associated with the 126, 82, 50, and 28 neutron shells. When the evaporation path crosses a neutron shell boundary the reduced neutron evaporation probability from nuclides with magic

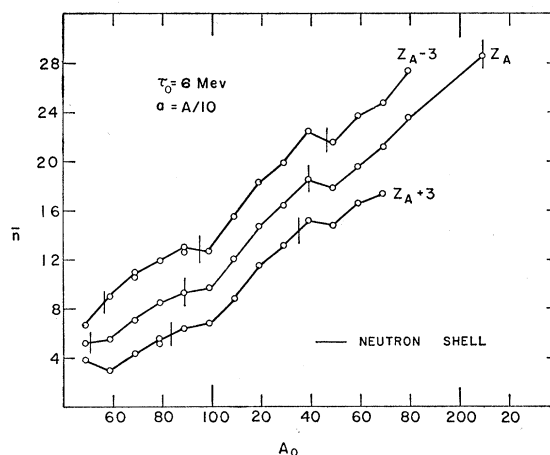


FIG. 6. Average number of neutrons evaporated from different starting nuclei. Initial temperature 6 Mev, $a=A/10$, $V=V_0$.

neutron number will depress the average number of neutrons evaporated in this particular cascade. This effect will occur in the evaporation of all nuclides with sufficient initial excitation to give products across the neutron shell below the starting nucleus. For the energies considered here the evaporation from a nucleus immediately below a closed shell will not cross the next shell down and therefore will not suffer the depression of the average number of neutrons which a neighbor a few mass units on the other side of the shell will undergo. It follows that the average number of neutrons emitted by such a nucleus will appear to be enhanced when compared with the value extrapolated from its heavier neighbors. It is interesting to note that the apparent enhancement is evident even for nuclei a few mass numbers on the high side of a shell. It is due to the fact that in the early stages of an evaporation cascade, when the temperature is still high, neutrons are not the most common evaporating particle. By the time neutron

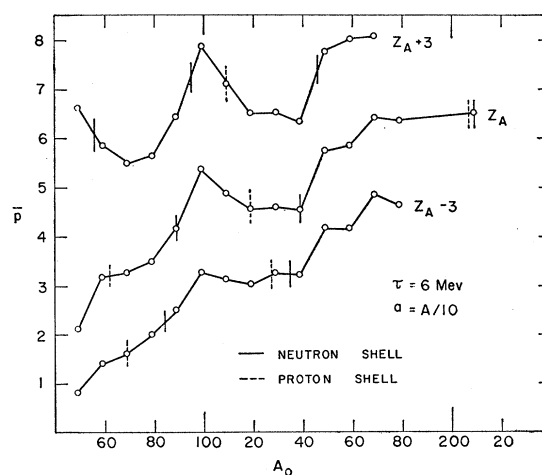


FIG. 7. Average number of protons evaporated from different starting nuclei. Initial temperature 6 Mev, $a=A/10$, $V=V_0$.

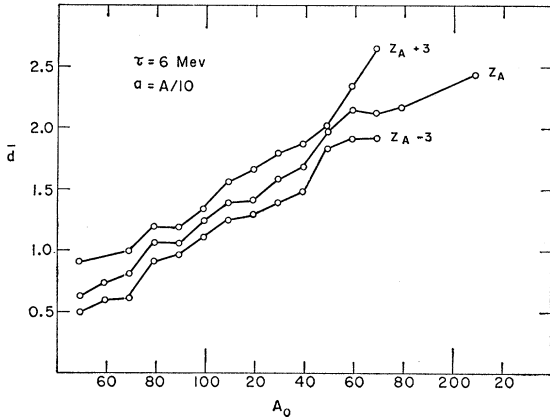


FIG. 8. Average number of deuterons evaporated from different starting nuclei. Initial temperature 6 Mev, $a = A/10$, $V = V_0$.

evaporation becomes the predominant process, the nuclei have crossed the shell and are not affected by it.

Neutron shells also have a profound effect on the evaporation of protons. In Figs. 5 and 7, prominent peaks in the average number of protons per cascade appear in the same mass regions as the breaks in the neutron emission plots. Since neutrons represent the majority of particles evaporated any depression of their emission will correspond to an increase in the probability of evaporation of all other competing particles. The sudden increase in the neutron evaporation when the original nucleus is taken below a neutron shell will correspond to sudden decrease in the number of other particles and particularly protons.

The situation for heavier particles is more complex still owing to the fact that the probability of their evaporation is also affected by the neutron shells, and in the same sense as the neutrons. A change in the neutron emission therefore does not lead to a great change in numbers of deuterons or alphas evaporated because of the partial cancellation of the effect by the changed probability of evaporating of the particles themselves.

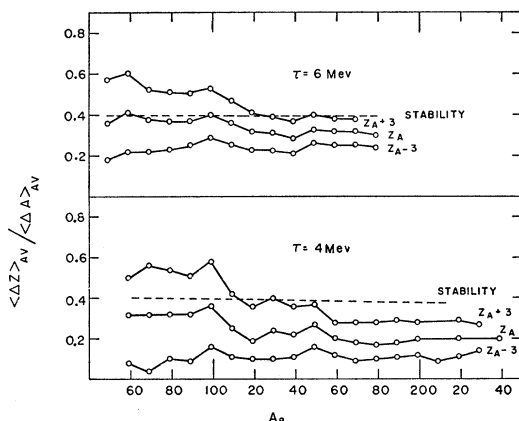


FIG. 9. $\langle \Delta Z \rangle_{AV} / \langle \Delta A \rangle_{AV}$ as a function of A and Z . $a = A/10$, $V = V_0$.

Another useful average property is the value of the over-all ratio $\langle \Delta Z \rangle_{AV} / \langle \Delta A \rangle_{AV}$ of the cascade, for it gives information regarding the coordinates, in the AZ plane, of the center of the distribution of the end products in terms of those of the starting nucleus.

In Fig. 9 are shown the values of $\langle \Delta Z \rangle_{AV} / \langle \Delta A \rangle_{AV}$ plotted against A for two values of the initial temperature. Shell effects are again evident. The values between shells are approximately constant. The approximate slope of the stability line is also drawn in (dotted line). Comparing values of $\langle \Delta Z \rangle_{AV} / \langle \Delta A \rangle_{AV}$ with the slope of the stability line, it is seen that at the lower temperature, in almost all cases the products are more neutron deficient than the initial nucleus. The exceptions are the neutron deficient nuclei below mass 110. At the higher temperature, all values of $\langle \Delta Z \rangle_{AV} / \langle \Delta A \rangle_{AV}$ are higher and therefore, again with the exception of neutron deficient nuclei below 120, the locus of the end product is more nearly parallel with the stability line. These facts are of course easily understood in terms of

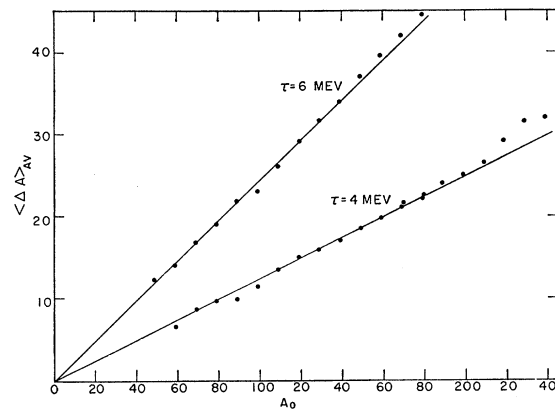


FIG. 10. Average number of nucleons lost as a function of mass of starting nucleus. $a = A/10$, $V = V_0$.

the increased probability of evaporation of charged particles at higher temperatures.

The approximate independence of $\langle \Delta A \rangle_{AV}$ on $(Z - Z_A)$ allows us to plot only one value of $\langle \Delta A \rangle_{AV}$ for each isobar in studying its dependence on A . Figure 10 is a plot of $\langle \Delta A \rangle_{AV}$ against A_0 for $\tau_0 = 4$, $\tau_0 = 6$ Mev. The approximate linear relationship of $\langle \Delta A \rangle_{AV}$ to A , disturbed somewhat by shell effects and in the high mass region suggests that the average de-excitation per nucleon for a given initial nuclear temperature is independent of A (and of Z) of the excited nucleus.

The average de-excitation per nucleon, ϵ , is composed of binding energy, Coulomb barrier, and the temperature dependent kinetic energy terms. As a consequence of the dependence of the proportion of charged particles emitted on the initial temperature, the contribution of the Coulomb barrier term will also vary with temperature. The over-all dependence of ϵ on initial temperature appears to be too complex to yield to quantitative

prediction. It is gratifying therefore to find that the computed values may be represented by a very simple linear relationship. In Fig. 11 are plotted the values of $\epsilon = E/\langle\Delta A\rangle_{AV}$ for Cu^{64} , Ag^{109} , Ta^{181} as a function of initial temperature. It is seen that the lines for the three starting nuclei are very close together and can be represented for most of their course by the equation

$$\epsilon = 8.9(\pm 0.15) + 0.97(\pm 0.025)\tau_0 \text{ Mev.} \quad (10)$$

From this expression it is possible to derive the value of the quantity $\langle\Delta A\rangle_{AV}/A$ for a given initial temperature. It is

$$\langle\Delta A\rangle_{AV}/A = c\tau_0^2/(8.9 + 0.97\tau_0), \quad (11)$$

where c is given by $a = cA$.

We may try and compute values of $\langle\Delta A\rangle_{AV}/A$ from

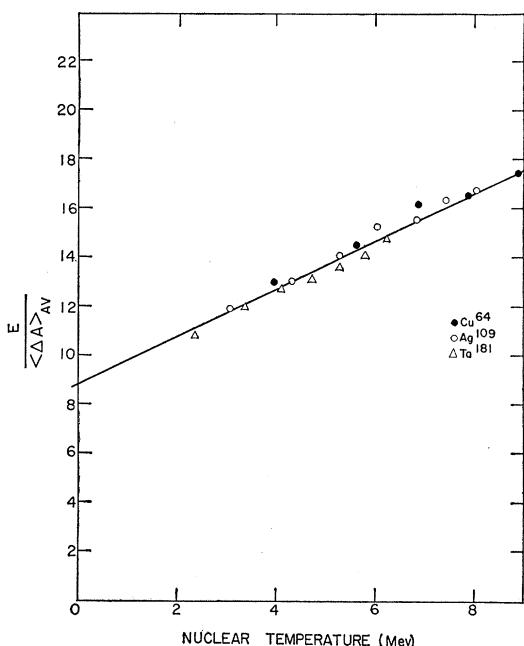


FIG. 11. Average de-excitation per evaporated nucleon as a function of initial nuclear temperature.

this equation and compare them with those obtained directly from the Monte Carlo calculation. Thus for $c=0.1$ and $\tau_0=4$ Mev, $\langle\Delta A\rangle_{AV}/A=0.124$ and for $\tau_0=6$ Mev, $\langle\Delta A\rangle_{AV}/A=0.243$. For $c=0.05$, the corresponding values are 0.062, 0.122. The lines corresponding to these values are plotted in Fig. 10. The extent of agreement between the lines computed from Eq. (11) and the values obtained directly from the computation is a measure of the accuracy of the assumptions embodied in Eq. (10).

The extent to which the assumption of the constancy of $E/\langle\Delta A\rangle_{AV}$ is justified is seen from Fig. 12 where the computed values of these quantities are plotted together with the lines representing the values for $\tau_0=4$ Mev and $\tau_0=6$ Mev computed from Eq. (10).

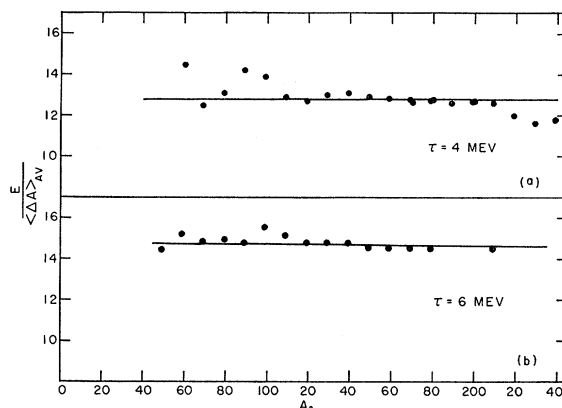


FIG. 12. Average de-excitation per evaporated nucleon as a function of initial mass of nucleus.

The ratio of tritons to He^3 emitted is very sensitive to the atomic number of the starting nucleus in a given isobar in the low mass region. In Fig. 13 this ratio is plotted against A of the isobars for values $Z=Z_A$ and $Z=Z_A+3$. This behavior of the ratio T/He^3 can be traced to the effect of the separation energy term Q [see Eq. (7)]. In the competition between He^3 and T emission from neutron deficient nuclei, the term Q is always in favor of the former because the product is then closer to stability. This effect is particularly strong in the low mass region where the sides of the stability valley are very steep. Also in this region the Coulomb barrier is weaker and the net result is that the favorable effect of Q (for He^3) more than compensates for the adverse effect of the Coulomb barrier as Z in the isobar is increased and the emission of He^3 becomes more probable. From Fig. 13 it is seen that the effect persists even in as high an isobar as 110 (for $Z=Z_A-3$). For starting nuclei closer to stability the ratio T/He^3 will be less than unity only for lighter isobars. The situation in the neutron excess part of the isobar is, of course, the precise converse, and in the lighter nuclei the emission of He^3 is strongly inhibited. In fact for almost all the Z_A-3 nuclei of isobars up to

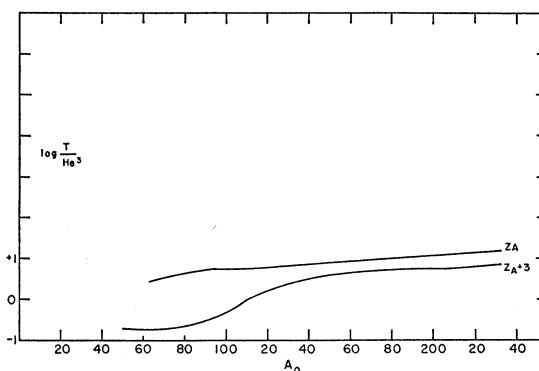


FIG. 13. The ratio of tritium to He^3 particles evaporated as a function of initial mass. Initial temperature 4 Mev, $a=A/10$, $V=V_0$.

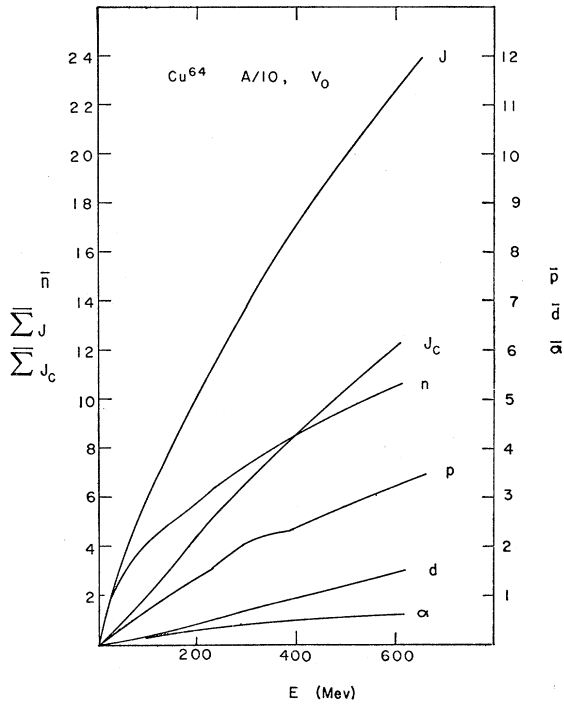


FIG. 14. The average number of neutrons, protons, deuterons, and He⁴ evaporated from Cu⁶⁴ as a function of initial excitation energy. $a=A/10$, $V=V_0$. Also shown are average numbers of particles (j) and charged particles (j_c) emitted.

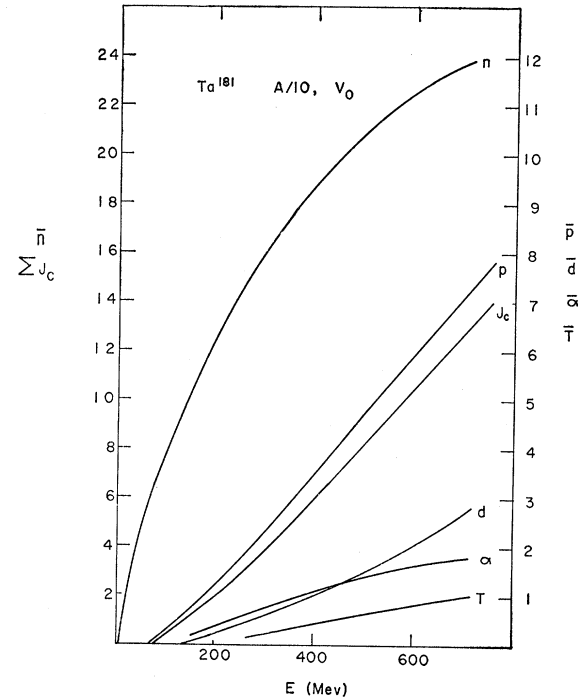


FIG. 16. The average number of neutrons, protons, deuterons, tritons, and He⁴ evaporated from Ta¹⁸¹ as a function of initial excitation energy. $a=A/10$, $V=V_0$.

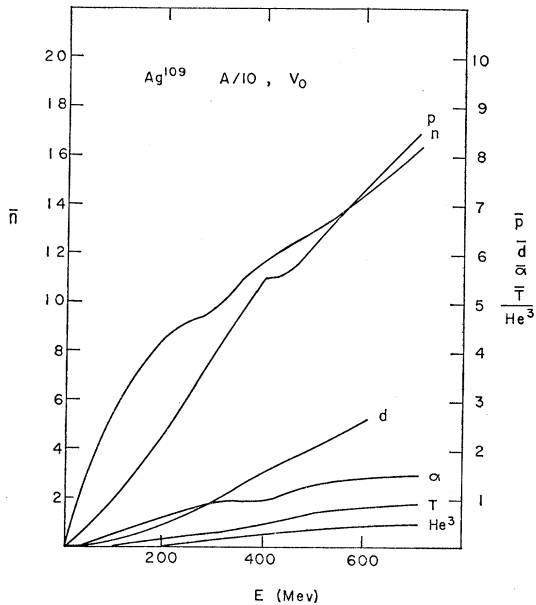


FIG. 15. The average number of neutrons, protons, deuterons, tritons, He³ and He⁴ evaporated from Ag¹⁰⁹ as a function of initial excitation energy. $a=A/10$, $V=V_0$.

about 100, no He³ particles were recorded in the 200 cascades computed for each case.

The irregularities introduced into the details of the evaporation process by nuclear shell structure make

any extrapolations beyond computed values uncertain. Even the close mesh of starting nuclei taken does not guarantee great precision in interpolation. To make extrapolation and interpolation somewhat easier and more accurate the data available from the calculations are analyzed in several different ways in the following pages.

It must not be forgotten, however, that all the calculations presented here refer to the idealized case of a given nucleus with a definite unique excitation. In any real experiment we deal of course with a range of nuclei each possessing a distribution of excitation energies. The actual behavior will be therefore a superposition of a large number of idealized properties such as are discussed here. Such a summation, properly weighted can be done readily by a computer, and examples of this will be presented in further papers. However, for rapid and approximate preliminary estimates of the results of certain experiments, the graphs given here when applied to proper average nuclei, and excitation energies, may be of some value.

VI. THE EFFECT OF INITIAL EXCITATION

From the comparison of the various characteristics of the evaporation cascades at the two initial temperatures of 4 Mev and 6 Mev, some general idea of the effect of initial excitation may be obtained.

More detailed investigation of the effect of initial excitation energy was carried out for certain nuclei selected as typical of certain regions of the table of

nuclides. These were Cu^{64} , Ag^{109} , and Ta^{181} . No heavier nuclides were chosen for this study for in them competition by fission can no longer be ignored. The fissile elements are discussed further in a forthcoming publication.⁷ In Figs. 14, 15, 16 are plotted the average numbers of the various types of particles emitted together with the averages of the total number of particles and charged particles, as a function of initial excitation energy. These plots may be compared with those of LeCouteur¹ with the difference that the parameters chosen by him were $a = A/12$ and a Coulomb barrier of 6 Mev with a temperature correction. In comparing our results with those of LeCouteur, it must be noted that the latter's results are in error due to the improper choice of the spin of the deuteron. This leads not only to considerable error in the proportion of deuterons emitted but also affects the yields of the other particles. The proportion of deuterons evaporated is seen to be quite high, and even for the heavier elements is above that of He^4 at the higher energies.

From Figs. 14-16 it is perhaps not so easy to see the way in which the relative proportions of the various particles change with initial excitation. In Fig. 17 is shown the average mass \bar{m} of the evaporated particles as a function of initial excitation. The increase in \bar{m} with E reflects the increasing proportion of heavier particles evaporated. In as much as all heavier particles are charged, the average charge per particle, \bar{z} , and per nucleon ($\langle \Delta Z \rangle_{AV} / \langle \Delta A \rangle_{AV}$) evaporated also increases. These characteristics are shown in Fig. 18. It is interesting, however, that the initial excitation has only a small effect on the ratio of singly to doubly charged particles (see Figs. 19 and 20).

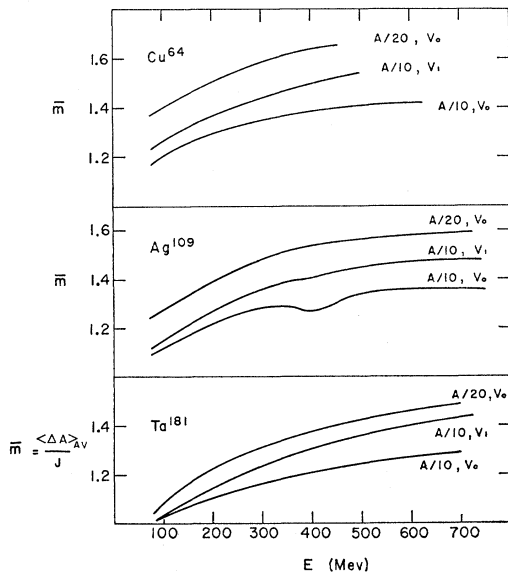


FIG. 17. Average mass of the evaporated particles as a function of initial excitation.

VII. TEMPERATURE CORRECTION OF THE COULOMB BARRIER

One of the more important parameters which enter the above computations is the Coulomb barrier for charged particle emission. Apart from the uncertainty introduced into the barrier formulation by the somewhat arbitrary choice of the nuclear radius parameter, r_0 , and the approximation of the penetration effect, both of which were described in Sec. II, a serious uncertainty remains regarding the effect of high nuclear

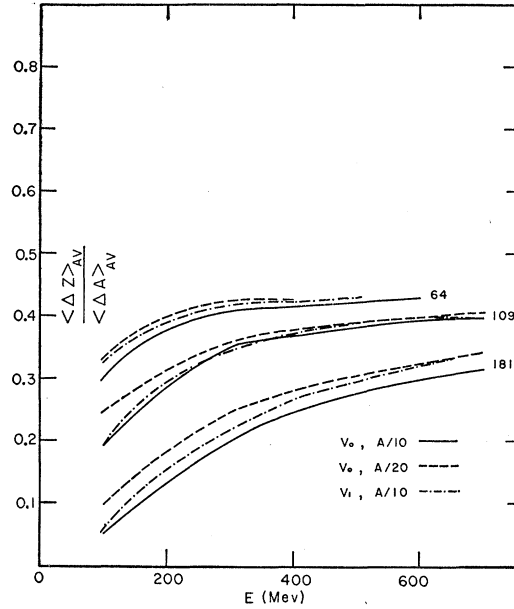


FIG. 18. $\langle \Delta Z \rangle_{AV} / \langle \Delta A \rangle_{AV}$ as a function of initial excitation for Cu^{64} , Ag^{109} , and Ta^{181} .

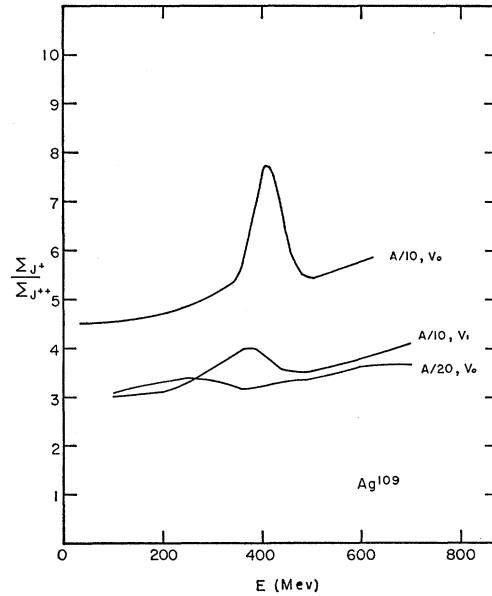


FIG. 19. Ratio of singly to doubly charged particles evaporated for Ag^{109} as a function of initial excitation energy.

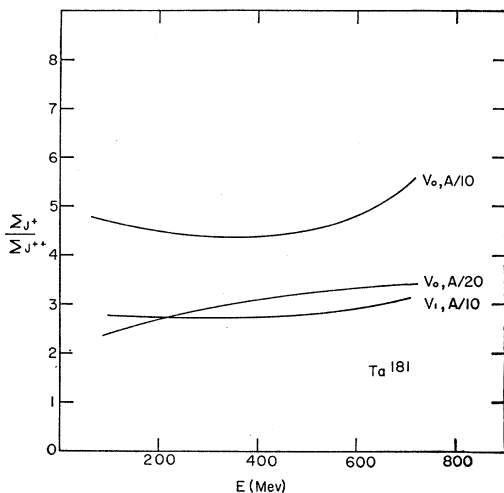


FIG. 20. Ratio of singly to doubly charged particles evaporated for Ta^{181} as a function of initial excitation energy.

excitation. Experimental evidence, mainly from nuclear emulsion work,^{17,18} suggests that at high excitations the value of the Coulomb barrier is reduced, and the effect has been interpreted in terms of nuclear thermal expansion and surface vibrations. The first is simpler to understand and a rough estimate of its importance has been made.²³ It amounts to about $0.8\tau^2\%$ change in radius and therefore in Coulomb barrier. The second effect has been discussed by Bagge²⁴ and its magnitude has been variously estimated as:

$$V = V'/(1 + 0.15\tau), \quad (\text{see reference 23}) \quad (12)$$

or

$$V = V'/(1 + E/\text{constant}), \quad (\text{see references 1, 5}) \quad (13)$$

where V' is a classical barrier corrected for penetration. The constant in Eq. (13) has been most frequently taken as 200 Mev.^{1,5}

In view of the uncertainty as to the need of the correction and its form, the present calculations were run with both corrected and uncorrected forms of the barrier (penetration correction was always applied). The correction formula used here was of the form

$$V = V'(1 - \tau^2/\tau_c^2), \quad (14)$$

where τ_c , a critical nuclear temperature, was taken as 9 Mev. This form of the correction was chosen for the sake of consistency with that applied to the fission barrier.^{2,7} If the fission process is assumed to be reversible, it follows that a correction applied to the barrier of the process should not depend on the direction from which it is considered (i.e., the same correction for fission and fusion reactions). Although the application of this argument to fission is doubtful,

²³ P. Morrison, *Experimental Nuclear Physics*, edited by E. Segrè (John Wiley and Sons, Inc., New York, 1953), Vol. II, p. 181.

²⁴ E. Bagge, *Ann. Physik* 33, 389 (1938).

in view of the general uncertainty prevailing regarding these corrections, the more consistent formula (14) was used. In magnitude, the correction is somewhat less severe than that used by LeCouteur [Eq. (13)] and more severe than that given by Eq. (12). The correction was taken as representing the net effect of both thermal expansion and surface vibrations.

A comparison of various average properties of the evaporation cascades calculated with and without barrier correction are shown in Figs. 21 and 22. It is seen from Fig. 21 that correcting the Coulomb barrier for initial excitation leads to only a slight increase in the average number of nucleons emitted per cascade

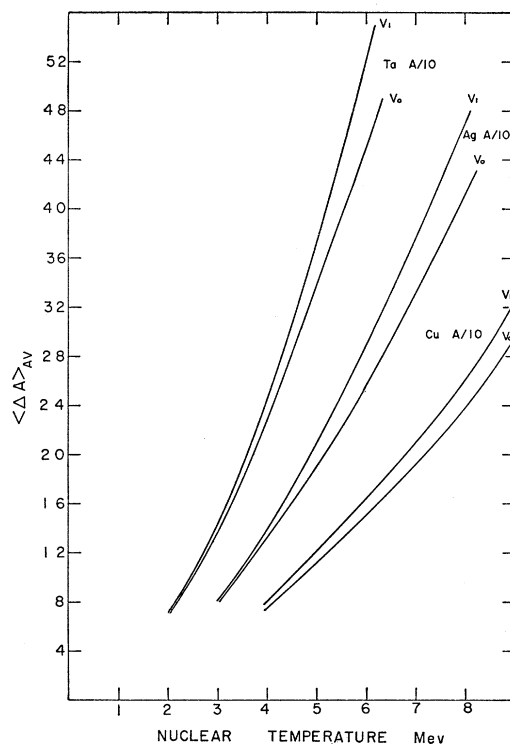


FIG. 21. Average number of nucleons evaporated from Cu^{64} , Ag^{109} , Ta^{181} as a function of initial excitation calculated with ($V=V_1$) and without ($V=V_0$) temperature dependence of the Coulomb barrier.

$\langle \Delta A \rangle_{AV}$). This in turn means that the average de-excitation per nucleon, ϵ , is not very sensitive to the assumptions regarding the Coulomb barrier dependence on excitation. This of course can be readily understood when it is recalled that the Coulomb barrier contributes only a part of ϵ and further, that the correction is only important in the early stages of the cascade. More remarkable is the fact that the average number of charged particles emitted per cascade (see Fig. 22) is also not very sensitive to the Coulomb barrier correction. Thus with the initial temperature of 4.5 Mev the Coulomb barrier for the early stages of the cascade is reduced to one half and yet the change in $\langle \Delta A \rangle_{AV}$ is

about 8% and is independent of A . Similarly the average number of charged particles emitted changes by 12% and the average number of charges lost, by about 14%. It follows that the value $\langle \Delta Z \rangle_{AV} / \langle \Delta A \rangle_{AV}$ is not particularly sensitive to the Coulomb barrier correction. The main effect of the correction is to change the ratio of singly charged to doubly charged particles emitted (see Figs. 19 and 20). Thus at 4.5-Mev initial temperature, this ratio changes from 4.3 uncorrected to 2.7 corrected for Ta¹⁸¹ and from 4.7 to 3.2 for Ag¹⁰⁹. The plot for Ag¹⁰⁹ illustrates again the powerful effect of the 50 neutron shell. The sharp rise in the ratio of singly charged to doubly charged particles between 300–500 Mev initial excitation is due to the high proportion of proton emission which in turn is due to the suppression

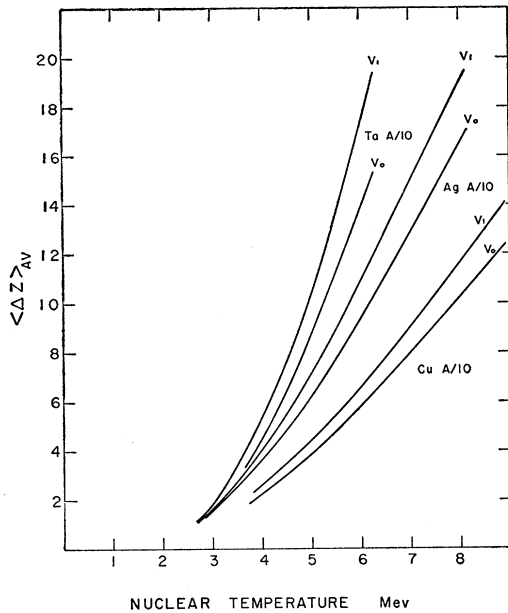


FIG. 22. Average number of charge units lost from Cu⁶⁴, Ag¹⁰⁹, Ta¹⁸¹ as a function of initial excitation calculated with ($V=V_1$) and without ($V=V_0$) temperature dependence of the Coulomb barrier.

of neutron evaporation in the shell region. At lower energies the evaporation path does not reach the shell. At much higher energies the relative importance of the shell effect is reduced owing to the larger number of particles lost and to the fact that most of the neutron emission occurs after the evaporation path had crossed the shell. A similar effect was observed in Cu⁶⁴, where the peak occurs between 200–400 Mev and is due to the 28-neutron shell (see Sec. V). The ratio of singly to doubly charged particles is of course related in a simple way to the emission ratio (ratio of doubly charged tracks to total tracks), used so much in nuclear emulsion work.

Experimental studies of ratios of singly charged to doubly charged particles, such as for example, the ratio

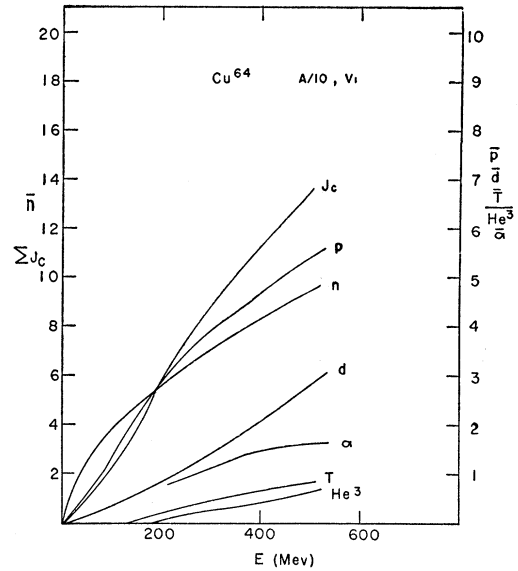


FIG. 23. The average number of neutrons, protons, deuterons, He³, He⁴, and charged particles evaporated from Cu⁶⁴ as a function of initial excitation energy. $a=A/10$, $V=V_1$.

of H³ to He³²⁵ should provide a useful check of the magnitude of Coulomb barrier correction necessary.

The proportions of the various particles emitted for Cu, Ag, and Ta when the Coulomb correction is applied are shown in Figs. 23, 24, 25 which may be compared with data of Figs. 14–16, which were computed without this correction.

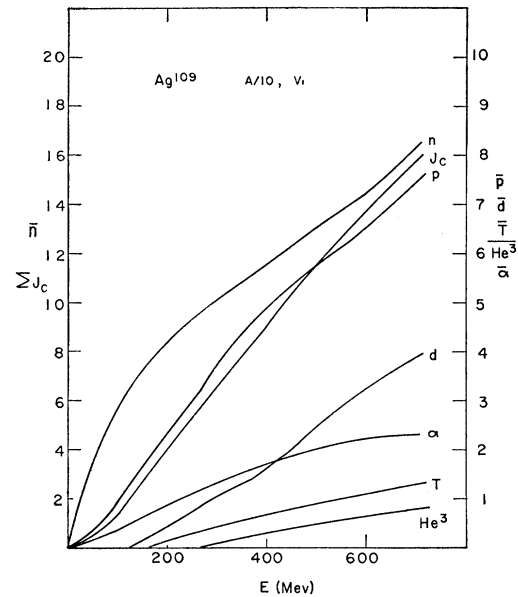


FIG. 24. The average number of neutrons, protons, deuterons, He³, He⁴, and charged particles evaporated from Ag¹⁰⁹ as a function of initial excitation energy. $a=A/10$, $V=V_1$.

²⁵ O. Schaeffer and J. Zähringer (private communication).

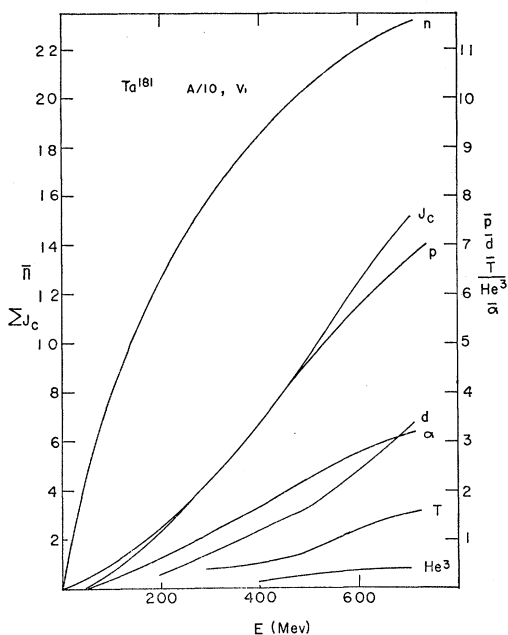


FIG. 25. The average number of neutrons, protons, deuterons, He^3 , He^4 , and charged particles evaporated from Ta^{181} as a function of initial excitation energy. $a=A/10$, $V=V_1$.

VIII. LEVEL DENSITY PARAMETER a

The uncertainty surrounding the proper function describing nuclear level densities at high excitations has already been discussed in Sec. II. Although most of the computations reported so far were carried out using the relationship $a=A/10$, a few runs were repeated using the value $a=A/20$. This was done in order to gain an appreciation of the quantitative effects of changes in a on the average properties of the evapo-

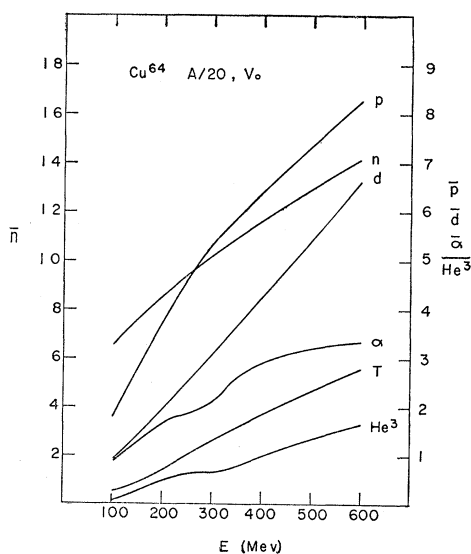


FIG. 26. The average number of neutrons, protons, deuterons, He^3 , and He^4 evaporated from Cu^{64} as a function of initial excitation energy. $a=A/20$, $V=V_0$.

ration process, so that when better values of a become available, the modifications which may be necessary to the results of our computations may be estimated.

As is seen from Eqs. (7), the effect of changing the dependence of a on A from $a=A/10$ to $a=A/20$ is equivalent to multiplying all the exponents by the factor 0.292 [$=1-(\frac{1}{2})^{\frac{1}{2}}$]. Since in most cases the exponent is negative this amounts to increasing the relative probabilities P_j/P_n . The increase will be greatest for the rarer particles (since they possess the most negative exponent), and small for protons. In some cases the exponent for protons is positive and of course there an actual decrease of the evaporation of this particle will result. In any case the increased probabilities of the evaporation of the rarer particles

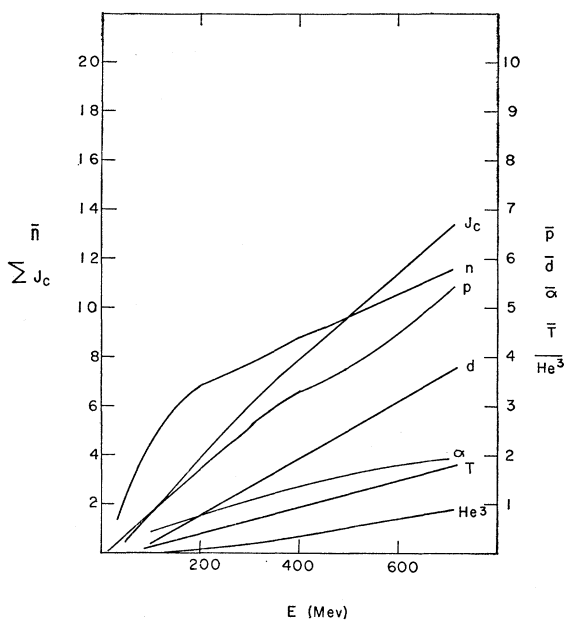


FIG. 27. The average number of neutrons, protons, deuterons, He^3 , He^4 , and charged particles evaporated from Ag^{109} as a function of initial excitation energy. $a=A/20$, $V=V_0$.

will usually result in a depression of the proportion of protons and neutrons. This of course is the same as saying that at higher nuclear temperatures the differences between particles (their Q 's and V 's) become less significant, with a corresponding tendency for equalizing their evaporation probabilities. These effects are clearly seen in Figs. 26, 27, and 28 when compared with Figs. 14-16.

The consequence of the increased evaporation probabilities of the rarer, and heavier, particles is that the average mass of the evaporated nucleon \bar{m} is higher with $a=A/20$ than with $a=A/10$. This is illustrated in Fig. 17. The effect on the number of charged particles lost and on total charges lost is expected to be small and of either sign, because of the mutually compensating increases in the rarer particles and the decrease

in protons. The ratio of singly to doubly charged particles will be affected in favor of doubly charged particles. For although the loss of protons may be compensated more or less by gain of other particles, the increase in He^3 and He^4 will lead to a decrease in the ratio $\sum J^+ / \sum J^{++}$. This effect is illustrated in Figs. 19 and 20. The "leveling" effect of the change to $a=A/20$ is also seen in Fig. 19 in comparing the curves for Ag^{109} —together with other quantities also the shell effect becomes of less significance.

In comparing the average number of nucleons lost, $\langle \Delta A \rangle_{Av}$, for the two values of a (see Fig. 29), a small decrease is noted in going from $a=A/10$ to $a=A/20$. This decrease is readily understood in terms of the average de-excitation per nucleon, ϵ . This quantity can

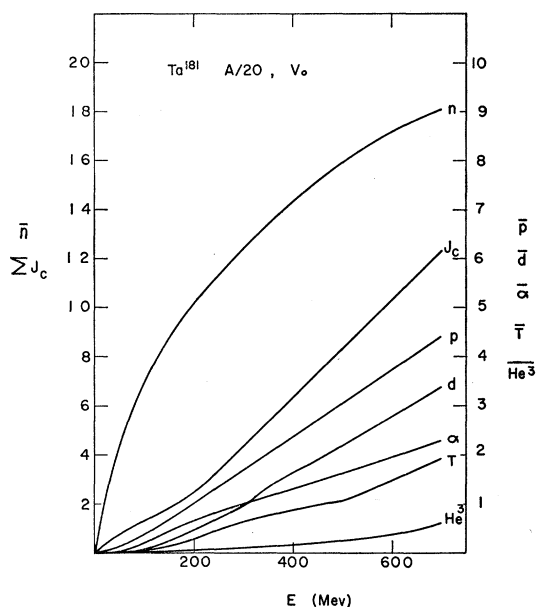


FIG. 28. The average number of neutrons, protons, deuterons, He^3 , He^4 , and charged particles evaporated from Ta^{181} as a function of initial excitation energy. $a=A/20$, $V=V_0$.

be written to a first approximation as

$$\epsilon = \bar{Q} + \bar{V} + 2\bar{\tau}, \quad (15)$$

where the various quantities are averaged over the whole evaporation cascade. The quantity $\bar{\tau}$, the average nuclear temperature, is the most sensitive to our choice of a , it is increased 1.4 times when a is changed from $A/10$ to $A/20$. Assuming \bar{Q} and \bar{V} do not change much, we may write for the ratio of the average de-excitation with the two values of a

$$\epsilon_{20}/\epsilon_{10} = 1 + 0.8\bar{\tau}/\epsilon_{10}. \quad (16)$$

For the highest excitation dealt with in this paper, the second term on the right may reach perhaps $\frac{1}{6}$. At the higher excitations therefore, A for $a=A/20$ will be expected to be some 15% lower than for $a=A/10$. The

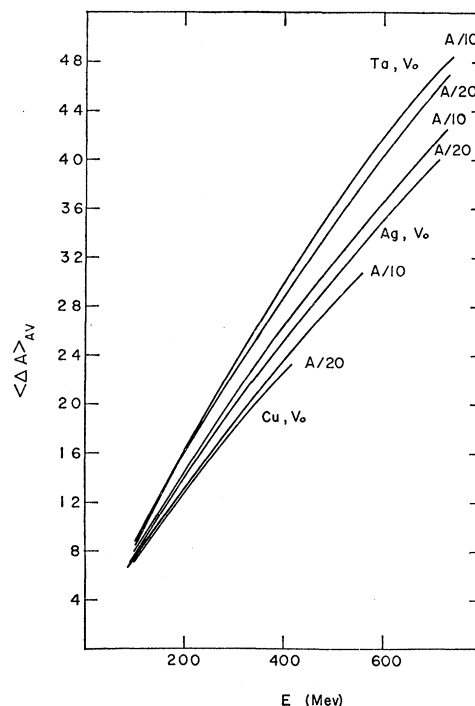


FIG. 29. Average number of nucleons evaporated from Cu^{64} , Ag^{109} , Ta^{181} as a function of initial excitation calculated for $a=A/10$ and $a=A/20$.

actual computed differences are 3% for Ta^{181} at 700 Mev and 6% for Ag^{109} at 700 Mev.

IX. ENERGY SPECTRA OF EMITTED PARTICLES

Experimentally, one powerful method of determining both the Coulomb barrier correction and the level density parameter is the study of the energy spectra of particles emitted in the high-energy bombardment of thin targets. A few such experiments are already available.²⁶ A computation which is suitable for direct comparison with experiment will have to take into account the results of the prompt cascade calculations.^{6,7} The evaporation computations of this paper have to be applied to the distribution of nuclei and excitations which result from the prompt knock-on cascade and also the contribution of particles emitted in those cascades must be added to the evaporation spectra. In the computation itself, a more accurate procedure has to be adopted in choosing the kinetic energy of the emitted particles. Such computations are now on hand and will be reported on later. However, it is of interest to examine the magnitude of the effects anticipated from changing the various parameters. In Figs 30–32 are presented a few of the average spectra from Ag^{109} obtained in the course of the preceding computations. Similar spectra are available for all nuclei studied in this paper. Although a Maxwellian

²⁶ R. W. Deutsch, Phys. Rev. 97, 1110 (1955).

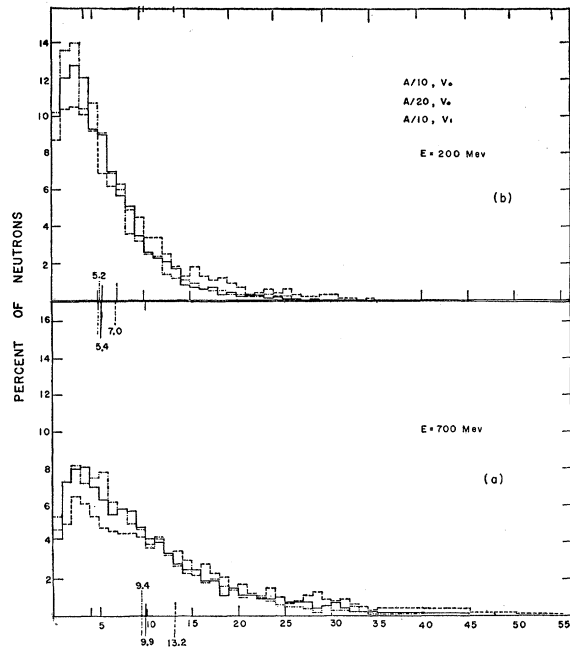


FIG. 30. Energy spectra of neutrons emitted from Ag^{109} calculated for various parameters. (a) 700-Mev initial excitation; (b) 200-Mev initial excitation. The short lines drawn on the abscissa represent the average values of the kinetic energy. In (b), $A/10, V_0$ is indicated by —; $A/20, V_0$ by - - -; and $A/10, V_1$ by - · - ·.

distribution was assumed for the kinetic energy of a given particle emitted from a given nucleus possessing a definite excitation energy, the computed final spectrum, being the sum of spectra for a range of nuclei and excitations, need no longer be simple Maxwellian.

Figures 31 and 32 show the expected displacement of the spectrum towards lower energies which results from the application of the Coulomb barrier correction. At the highest initial excitation this displacement is equivalent to a reduction of the average barrier of 2–3 Mev for protons and about double that amount for alphas.

Charged particles which are emitted toward the end of the evaporation cascade are subjected to a smaller Coulomb barrier than those emitted initially because of the loss of charges from the initial nucleus. This effect will be more important for long evaporation cascades (high initial excitation) than for the short ones. Accordingly we find that the spectra of particles from highly excited nuclei contain not only a higher proportion of high-energy particles, as is to be expected from the higher average temperature, but also a higher proportion of low-energy particles. This effect is clearly discernible in comparing the spectra of protons and alphas for the two excitation energies.

The average kinetic energies obtained in the computation for the particles and parameters shown in Figs. 30–32 are also plotted there as short vertical lines.

It is of interest to study the relation between the average kinetic energy and the mode of the spectra as a guide to the extent to which the spectra still obey the simple Maxwell distribution assumed for the discrete evaporation probability. Taking the neutron spectrum first (Fig. 30), we find for 200-Mev initial excitation the mode to be between 2–3 Mev, while the average is 5.4 Mev, i.e., twice the mode. The spectrum satisfies then this criterion of a Maxwell distribution. On the other hand, in the 700-Mev spectrum, the mode is about 3 Mev while the average is 9.9 Mev, and the ratio of the latter to former is far from 2, the value expected for a

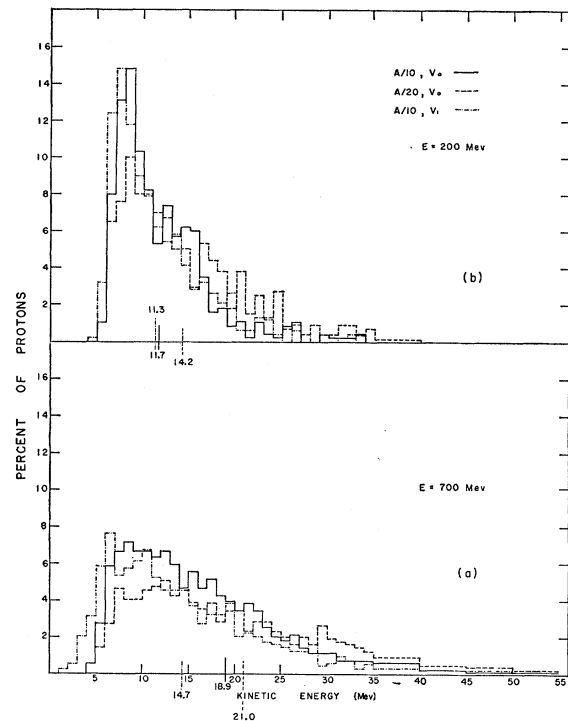


FIG. 31. Energy spectra of protons emitted from Ag^{109} calculated for various parameters. (a) 700-Mev initial excitation; (b) 200-Mev initial excitation. The short lines drawn on the abscissa represent the average values of the kinetic energy.

Maxwellian. This difference between the high- and low-initial-excitation spectra is due to the much wider distribution of emitting nuclei, both in kind and in excitation, in the former case. A similar situation is found in the proton spectra. The 200-Mev initial excitation spectrum has a mode between 8–9 Mev and an average value of 11.7. Subtracting the Coulomb barrier from these (4.8 Mev), we obtain 3–4 for corrected mode and 7 for corrected average kinetic energy, and again the approximation to a Maxwellian (displaced by the Coulomb barrier) is satisfactory. For the 700-Mev spectrum the values obtained in a similar way are 3–4 Mev and 14 Mev, again far from the expected ratio for a Maxwellian.

The non-Maxwellian form of the spectra from the highly excited nuclei makes it impossible to assign values of the average temperature during the evaporation process on the basis of particle spectra. For the lower initial excitation this procedure is more justified. In such cases it should be noted that the average temperature deduced from the neutron spectrum will differ from that deduced from proton or from alpha spectra. This arises from the fact that the different particles sample different parts of the evaporation cascade. While the neutrons are averaged for the whole process, protons and alphas are more common in the early parts of the cascade and therefore sample a population which

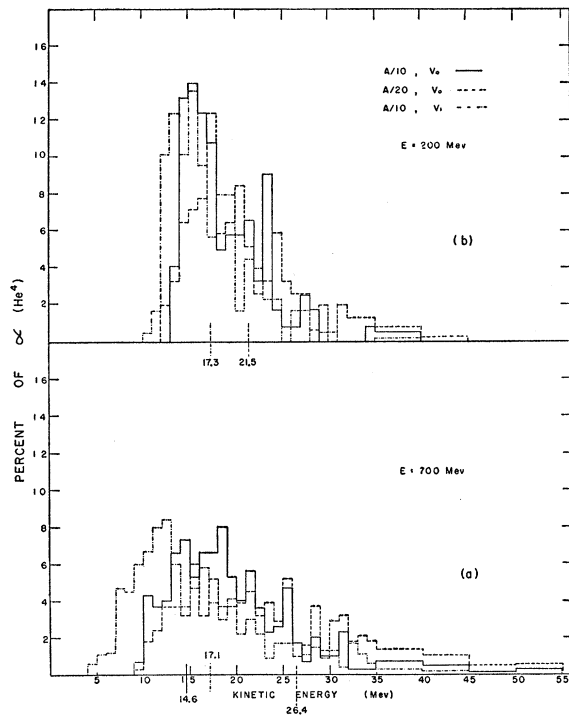


FIG. 32. Energy spectra of alpha particles emitted from Ag^{109} calculated for various parameters. (a) 700-Mev initial excitation; (b) 200-Mev initial excitation. The short lines drawn on the abscissa represent the average values of the kinetic energy.

is somewhat "hotter" on the average than that sampled by the neutrons. The discrepancy between average temperature obtained from neutron spectra and that from charged particles will be more serious for the heavy nuclei with their higher Coulomb barriers.

The effect of a can be seen in comparing the spectra of Figs. 30-32. The general flattening of the spectrum for the smaller values of a is quite marked and therefore the experimentally observed shape of the spectrum should provide fairly sensitive check on the correctness of a chosen for the computation. In this way it may be possible to arrive at an estimate of a at high excitations

TABLE IV. Distribution of products from the evaporation of Ag^{109} excited to 400 Mev. ($a=A/10, V=V_0$.)

$Z \backslash A$	33	34	35	36	37	38	39	40	41
73	2	1							
74									
75		1							
76		2		1					
77		1	2						
78		1	2	4					
79			2	10	2				
80				14		6			
81				4	10	1			
82			1	7	6	21			
83					5 ^a	21			
84					1	21	3		
85					1	9	13		
86						5	4	8	1
87							1	4	
88								2	
Totals	2	6	7	40	25	84	21	14	1

^a Center of distribution as calculated from $\langle \Delta Z \rangle_{Av}$ and $\langle \Delta A \rangle_{Av}$.

and to study its dependence on initial excitation and initial A and Z of the nucleus.

X. FLUCTUATION

The statistical nature of the evaporation process leads to fluctuation in the numbers of various particles emitted and to a distribution of the final products. The center of this distribution is given of course by the value $\langle \Delta Z \rangle_{Av} / \langle \Delta A \rangle_{Av}$. A sample of such a distribution of products obtained from Ag^{109} excited to 400 Mev is given in Table IV. These distributions show shell effects and also fine structure due to the odd-even effect on nuclear stability. For these reasons it is not very useful to make generalizations regarding these distributions except to point out the elliptical shape which is quite generally observed.

The fluctuation in the number of particles emitted was investigated in a few runs by modifying the program so as to print out the numbers of the various particles emitted in each cascade. These were then analyzed statistically and their distribution about the mean determined. It was found to be much sharper than the Poisson distribution. For example, the number of neutrons emitted from Hg^{199} at 318-Mev initial excitation is 17.75 ± 1.68 while that from Xe^{129} at 205 Mev excitation is 10.05 ± 1.32 . These results differ considerably from the approximate estimates obtained by Fujimoto and Yamaguchi² which predict a distribution closer to a Poissonian, and illustrate the severe distortion which the various simplifying assumptions introduce. From the standard deviations given above, it is possible to compute by well-known formulas the standard deviation of the means of groups of 200 cascades. These turned out to be 0.12 and 0.094 respectively for the two cases given above, and can serve as a measure of the precision of the points calculated in this paper.

ACKNOWLEDGMENTS

This work was initiated while the senior author was a guest at Brookhaven National Laboratory. He wishes to record his appreciation of the hospitality accorded to him by the Chemistry Department and to acknowledge the many fruitful discussions with Dr. G. Friedlander.

The authors also wish to thank Dr. Z. Fraenkel for many useful discussions and comments during the preparation of the manuscript, and the operating crews of the MANIAC and WEIZAC computers for the many hours devoted to these computations, often at odd times.

 π^- - p Interactions at 1.85 Bev/ c^\dagger

R. C. WHITTEN* AND M. M. BLOCK
Duke University, Durham, North Carolina
 (Received May 29, 1958)

This paper reports some diffusion cloud chamber results concerning the elastic and inelastic scattering in hydrogen of pions having a momentum in the laboratory system of 1.85 Bev/ c . The elastic scattering data are consistent with diffraction by a sphere of radius 0.85 f and opacity 0.9. The forward scattering amplitude was found to be in agreement with that derived from the dispersion relations. Investigation of the inelastic scattering disclosed that there is little agreement with the predictions of the Fermi statistical model. The angular and Q value distributions of the particles emerging from inelastic interactions showed little agreement with either the statistical theory or the excited isobar model.

I. INTRODUCTION

THIS paper reports results of π^- - p scattering at an incident pion momentum of 1.85 ± 0.2 Bev/ c . Three investigations of π^- - p interactions in the 1.0 to 1.5 Bev range using pion beams at the Brookhaven Cosmotron¹⁻³ and two in the range 4.5 to 5.0 Bev using pion beams at the Berkeley Bevatron^{4,5} have been conducted. The present investigation utilizes the most energetic pion beam available at the Brookhaven Cosmotron.

In this experiment a negative pion beam was directed through a hydrogen filled diffusion cloud chamber. The resulting interactions were analyzed for the elastic fraction, multiplicity of pion production, charge-state distributions for a given multiplicity, and pion and nucleon momenta in the center-of-mass system.

The objectives of the experiment were as follows:

1. To investigate the angular distribution of the elastically scattered pions. The occurrence of inelastic interactions leads to diffraction scattering, the angular distribution of which is related to the size and opacity of the proton.

2. To investigate the multiplicity of pion production. A comparison of the number of cases in which 0, 1, 2,

and 3 secondary pions are produced is made with the Fermi statistical theory.

3. To investigate the momentum, angle, and charge states of emitted particles. This information should also shed light on the validity of current theories of pion production.

4. To investigate Q -value distributions of nucleon-pion pairs. Information resulting from these data should be helpful in determining the existence or nonexistence of an excited isobar ($J = T = \frac{3}{2}$).

II. EXPERIMENTAL PROCEDURE

Protons accelerated to a kinetic energy of 2.95 Bev by the Cosmotron, which was pulsed once every seven seconds, were allowed to strike a carbon target. Those π^- mesons which were emitted in the forward direction were deflected about 20° by the Cosmotron fringing magnetic field and were allowed to pass through a 2 inch by 12 inch channel in the Cosmotron shield. A steering magnet then deflected 1.85-Bev/ c pions through a channel in the cloud chamber blockhouse into the hydrogen-filled cloud chamber, which was operated at 20 atmospheres in a magnetic field of 10 500 gauss. The momentum band accepted was 1.85 ± 0.2 Bev/ c . The Cosmotron beam intensity was adjusted so that a typical beam pulse contained about 15 pions which crossed the chamber.

Approximately 19 000 stereoscopic pairs were photographed and scanned for interactions. Angles in space with respect to the incident pion track were measured using a stereoprojector.⁶ Particle momentum was

[†] This work was supported in part by the joint program of the U. S. Atomic Energy Commission and Office of Naval Research.

* This paper is based on a thesis submitted in partial fulfillment of the requirements for the degree of Master of Arts in the Graduate School of Arts and Sciences of Duke University.

¹ Walker, Hushfar, and Shepard, Phys. Rev. **104**, 526 (1956).

² Eisberg, Fowler, Lea, Shephard, Shutt, Thorndike, and Whittemore, Phys. Rev. **97**, 797 (1955).

³ W. D. Walker and J. Crussard, Phys. Rev. **98** 1416 (1955).

⁴ Maenchen, Fowler, Powell, and Wright, Phys. Rev. **108**, 850 (1957).

⁵ W. D. Walker, Phys. Rev. **108**, 872 (1957).

⁶ Fowler, Shutt, Thorndike, and Whittemore, Rev. Sci. Instr. **25**, 996 (1954).